Green production of biologically active Ag and Ag-Cu nanoparticles from Prosopis cineraria pod waste extract and their application in epoxidation

Prashant Kumar
CSIR-Central Institute of Medicinal and Aromatic Plants (CSIR- CIMAP)
Praveen Kumar Sharma
CSIR-Central Institute of Medicinal and Aromatic Plants (CSIR- CIMAP)
Shivani Chaturvedi
CSIR-Central Institute of Medicinal and Aromatic Plants (CSIR- CIMAP)
Suman Singh
CSIR-Central Institute of Medicinal and Aromatic Plants (CSIR- CIMAP)
Shreya Tripathi
Indian Institute of Technology
Huma Fatima
Indian Institute of Technology
Minakshi Grover
ICAR- Indian Agricultural Research Institute
Priyabrat Mohapatra
C.V. Raman Global University
Chandan Singh Chanotiya
CSIR-Central Institute of Medicinal and Aromatic Plants (CSIR- CIMAP)
Prasant Kumar Rout (pk.rout@cimap.res.in)
CSIR-Central Institute of Medicinal and Aromatic Plants (CSIR- CIMAP)

Research Article

Keywords: Ag NPs, Ag-Cu NPs, Prosopis cineraria, Epoxidation, antimicrobial activity

Posted Date: September 6th, 2022

DOI: https://doi.org/10.21203/rs.3.rs-2016614/v1

Abstract

Bio-nanotechnologically produced nanoparticles (NPs) utilizing waste materials have been the main focus of the current research. There is a need for developing an advanced technology to reduce waste in an eco-friendly way. Therefore, presently the discarded aqueous portion of *Prosopis cineraria* pods was used after boiling to synthesize Ag and Ag-Cu NPs. FT-IR spectra illustrated the presence of phenyl propenoids and flavonoids were displaying capping and reducing properties. TEM and SEM imaging exhibited an average size of Ag NPs (14 nm) and Ag-Cu NPs (27 nm). The crystallinity nature was confirmed by XRD, and the Cu in Ag-Cu NPs was validated through energy dispersive X-ray analysis. According to the antimicrobial data, *Saccharomyces cerevisiae* displayed a zone of inhibition (ZOI) of 42.85% (Ag NPs) and 33.98% (Ag-Cu NPs) at lower concentrations (0.0321 mg/ml), while *Bacillus subtilis* was found most susceptible (85% ZOI) to Ag NPs at 0.5 mg/ml concentration. Further, these NPs (Ag and Ag-Cu) were utilized in the epoxidation of alkene moieties. Ag NPs showed lower conversion (65%) while, Ag-Cu NPs were very active for epoxidation of linalool (93% conversion), suggesting the presence of Cu was facilitated epoxidation. To the best of our knowledge for the first time, the aqueous waste was applied to prepare green NPs for using as antimicrobial agents and synthesis of platform chemical (epoxide) for industrial aspects. These inexpensive ways of producing green NPs is utilized several times and have found potential applications in nano-medicine, therapeutics, modification of monoterpenoids to fine fragrance, etc.

Introduction

Synthesis of nanomaterials is an emerging field of nanotechnology [1], particularly with a greener approach to the metallic nanoparticle (NPs), a crucial nanobiotechnological research area [2]. Several chemicals, physical, and biological approaches to NPs synthesis have been attempted, but the biological approach (bacteria, plants, and fungi) appeared to fastest, cost-effective, and environment-friendly [3]. Green NPs synthesis from plant waste offers economical, and safer waste management alternative. There have been several works on synthesizing NPs from plant components, but no studies on plant waste material-generated NPs have been done. In this context, *Prosopis cineraria* (L) (commonly called ‘Sangri’) popularly grown in the arid and semiarid regions is explored. *P. cineraria* was used in leukoderma, hyperglycemia, and hypercholesteremia and also possessed antimicrobial and anticancer activities [4]. In the traditional Indian cuisine of the native desert area, *P. cineraria* were prepared by overnight soaking, washing, and boiling of pods. The wastewater extract of overnight soaking was earlier reported for inhibiting the main enzyme 3-hydroxy-3-methyl-glutaryl reductase in the mevalonate pathway [5]. This reduces ergosterol, carotenoids and increases triglyceride (TAG) biosynthesis. In the traditional recipe, after soaking overnight, the wastewater was discarded and the pods are washed many times with water. In the current study, from this wastewater, Ag and Ag-Cu NPs were prepared which act as an excellent capping agent.

The naturally synthesized NPs were earlier reported to have antimicrobial activity [6], and Ag NPs were widely used in cosmeceuticals, textile manufacturing, water purification, apoptotic response in human

cells, and cancer treatment, with no adverse side effects [7]. Cu NPs were also utilized in clinical therapy, cervical cancer, and wound healing [8]. Greener metallic NPs are limited in the commercial market, so preparing them by environmental-friendly and cost-effective process is the need of the hour. Capping agents were needed to stabilize NPs either from petrochemical origin or natural products.

The aim of this research work is to employ a green capping agent, the *P. cineraria* pod waste water extract was found beneficial due to its wide spectrum of natural molecules (flavonoids and polyphenols) which avoid particle overgrowth and aggregation during NPs synthesis [9]. From the present work, the NPs synthesized from *P. cineraria* waste water is further used in the epoxidation of monoterpenes like linalool and limonene to give an industrially relevant pharmacological precursor. The cyclized and epoxide products were huge importance in various drug syntheses [10, 11]. Therefore, this study focused on an exploration of waste materials for the production of NPs possessing antimicrobial activities. In addition, these NPs are selectively oxidized the monoterpenes to monoterpene epoxides economically for various commercial applications.

Experimental

Materials and Methods

Silver nitrate ($AgNO_3$), copper acetate (Cu $(CH_3COO)_2$), and sodium hydroxide (NaOH) were purchased from Merck, Mumbai, India. All cell culture media were supplied by Hi-Media, Mumbai, India. The double-distilled water was utilized for the synthesis of Ag and Ag-Cu NPs in the present study.

Prosopis cineraria pod extract preparation

To prepare the crude extract, *P. cineraria* pods (10 g) were thoroughly rinsed and washed. The pods were boiled for 2 h at 80 °C in 100 ml of de-ionized water. The extract solution was filtered and then stored at 4 °C for the biosynthesis of Ag and Ag-Cu NPs.

Green synthesis of Ag and Ag-Cu NPs

To synthesize Ag-Cu NPs, 10 ml of *P. cineraria* extract, 25 ml of an aqueous copper acetate solution (2 mM) and 75 ml of an aqueous silver nitrate solution (10 mM) was added simultaneously under stirring for 3 h at 90 °C. Light brown to black colour change indicated the formation of the bimetallic Ag-Cu NPs. The precipitate was purified by centrifuging at 10,000 rpm for 30 min at 25 °C. The centrifuged particles were then washed three times with ethanol to follow double-distilled water and dried at 120 °C in a vacuum oven in order to get the final nanopowder. Cu NPs and Ag NPs were also synthesized separately in order to endorse the higher impact of bimetallic Ag-Cu NPs on antimicrobial and cytotoxic potential over monometallic nanomaterials. Cu NPs were synthesized by adding a 100 ml of aqueous copper acetate solution after mixing with 10 ml of *P. cineraria* extract.

Characterization of NPs

The NPs were characterized using SEM, TEM, XRD, FT-IR, and UV-Vis analysis. A UV-Vis spectrometer (model number UV-245 Shimadzu) was used to visualize the surface plasmon peak of the Ag-Cu NPs. A quartz cell with a path length of 1 cm was loaded with few drops of fresh solution containing biosynthesized Ag-Cu NPs, and the cell was scanned in the wavelength range of 200-700 nm. The XRD spectra of the composites were recorded through Rigaku diffractometer (Rigaku, Japan) by using Cu Ka radiation at 40 kV and 130 mA in the scanning angle of 5-50^{o} at 0.05^{o} scanning speed. The spectra are presented with the 2θ Vs. intensity. FT-IR spectra of samples were acquired using Nicolet 138 400D-Impact FT-IR spectrophotometer. The method used was the KBR pellet method, and the region that analyzed was 4000-500 cm^{-1} at a resolution of 4 cm^{-1}. After applying 10,000 hydraulic pressures for 2-3 min, the dry KBR of 200 mg and the sample of 5 mg were well mixed to create pellets. Each sample was scanned 200 times, and the wave number against transmittance (%) was used for recording the spectra. The QUANTA-250, FEI (Netherlands) SEM equipment was utilised in order to conduct morphological study of the NPs. Samples (50 mg) have been coated with gold by Sputter Coater for 50 s (Model 147 No: Q150 TES frocoram Technology, U.K). Sputtering with silver was used to create layers on the NPs. The instrument was kept at 20 kV for determining the particle size and shape of the NPs. TEM was performed by using an electron microscope with a filament as a source of electrons operated at 300 kV. TEM imaging and mapping were carried out by using Field Emission Gun-Transmission Electron Microscope 300 Kv (TEM 300 kV), FEI, Tecnai G2, F30.

Antimicrobial activity

Kirby Bauer disc diffusion method was used to observe the antimicrobial activity [12]. Fresh inoculum (100 µL of 10^{7} cfu) of *Saccharomyces cerevisiae, Escherichia Coli, and Bacillus subtilis* was spread onto the Mueller Hinton agar plates and dilution of 10 µl stock solution of Ag and Ag-Cu NPs, gentamycin (standard), and water (negative control) was impregnated into a disc and placed in the Petri plate. After incubation for 24 h at 37 °C, the inhibition zone was observed and calculated by comparing it with the negative control.

Epoxidation reaction

Typically, epoxidation of monoterpenes was employed by both NPs using an environmental-friendly oxidant H_2O_2 to investigate the catalytic activity. For this, linalool was taken as a substrate in order to optimize the reaction condition of alkene epoxidation and reacted with hydrogen-peroxide in presence of NPs. The effect of Ag NPs and Ag-Cu NPs in linalool epoxidation was studied in following operating conditions as linalool: hydrogen peroxide (1:2), 20 ml acetonitrile, 0.1% AcOOH at 50 ^{o}C. The reaction products were monitored by GC-FID and GC-MS. The final products were extracted in diethyl ether and the NPs were separated out through filtration, washed numerous times, and calcined at 400 ^{o}C for 4 h.

The conversion is determined by using the Eqs. (1-2).

$$XCAL = \frac{Ccal^o - Ccal^t}{Ccal^o} \quad \text{..... Eq. 1}$$

where $Ccal^o = initial\ concentration$, and $Ccal^t = concentration\ at\ time\ t$

Product selectivity (Si) is calculated as $Si = \frac{Ci}{\sum Ci}$ ..... Eq. 2

$$\sum Ci = total\ moles\ of\ product$$

Results And Discussion

In the current study, *P. cineraria's* pod waste water extract was first time utilized to make Ag and Ag-Cu NPs. The waste water showed high reducing and capping abilities. The overall process of NPs synthesis is given in Scheme 1. The different waste waters are generated during the process of Sangri-dish preparation listed in Table 1 and Fig. 1 to synthesize Ag and Ag-Cu NPs. It has been observed that washed and boiled *P. cineraria* waste water yielded the maximum precipitate, i.e., 458 mg (Ag NPs) and 710 mg (Ag-Cu NPs). Before synthesis, both NPs solutions were light yellow, but turned brown after 2 h, and olive-green precipitates formed, indicating the successful formation of NPs (Fig. 1). Pod extract of *P. cineraria* can be used in NPs synthesis as it contained several plant metabolites such as flavonoids and phenolics [5]. These properties minimized as well as stabilized the metals preventing particle agglomeration [13]. Table 2 showed a comparative study of reported NPs synthesis using natural materials with the present prepared method.

Characterization of Ag and Ag-Cu NPs

UV-Vis analysis

UV-Vis spectra in the range of 300-700 nm are confirmed the formation of NPs with broad single SPR (surface plasmon resonance) peaks (Fig. 2A). A single SPR peak around 420 nm matches the λ_{max} of Ag NPs, which is in correspondence with the report of Manjari et al. [14]. For bimetallic NPs, if the metals combine to form alloys, a single SPR peak is observed whereas a core shell-like structure is displayed with two distinct peaks. In the current study, only a single SPR peak around 426 nm for Ag-Cu suggested the formation of the alloy structured NPs [15].

FT-IR analysis

FT-IR spectra showed functional groups in both NPs (Fig. 2B). Intensive vibrations are obtained at the band positions of 602 cm^{-1}, 1061 cm^{-1}, 1312 cm^{-1}, 1621 cm^{-1}, 2106 cm^{-1}, 2853 cm^{-1}, 2921 cm^{-1}, 3175 cm^{-1}, 3334 cm^{-1}. The peaks at 3334 cm^{-1} and 3175 cm^{-1} indicated O-H and O=CH stretching respectively, at 2921 cm^{-1} and 1621 cm^{-1} to C-H stretching of alkanes and -C=O vibrations respectively, 1061 cm^{-1} is all-trans C-C asymmetric stretching respectively, 1096 cm^{-1} is gauche skeletal C-C stretching. While 2800-

3000 cm^{-1} is C-H stretching vibrations, therefore, the band at 2853 cm^{-1} could be considered for CH_2 symmetric stretching. Further, the λ_{max} at 1358 cm^{-1} is of a CH_2 wagging band [16], while 820 cm^{-1} is due to symmetric C-O stretching [17].

XRD analysis

The XRD diffractogram for both NPs are shown in Fig. 2C with 2θ values in between 10° and 90°. Fig 2C showed the scattering peaks of 38° (111), 44° (200), 64° (220), 77° (311), 43°. These diffraction peaks characterization agreed with Akintelu and Similoluwa [18], Periyasamy et al. [6]. Both NPs possessed high crystalline nanostructures, the average size was calculated using Debye-Scherer equation [19]. The average values were 14 nm (Ag NPs) and 27 nm (Ag-Cu NPs), respectively. Further, the size was correlated with TEM analysis, and the values were well matched with the standard JCPDS. Due to Ag-Cu NPs is contained low Cu, hence, no distinct peak of Cu is observed. Furthermore, the broadening peaks of Ag-Cu NPs in comparison with Ag NPs is revalidated the presence of Cu and its fair incorporation in the synthesized NPs.

SEM-EDAX analysis

Fig. 2D-D1 and Fig. 2E-E1 showed the EDAX spectra for both NPs. In Ag-Cu NPs, silver, copper, and oxygen are present with a greater weight percentage of Ag and Cu. In Ag NPs, silver, carbon, and oxygen are present with a higher weight percentage of Ag. The signal of Ag from the EDAX spectrum in Ag NPs, and both Ag and Cu from the EDAX spectrum of Ag-Cu NPs confirmed the successful formation of respective NPs.

TEM analysis

The images illustrated the spherical shape and the dispersed nature of NPs (Fig. 2F and 2G), where the spherical shape is due to phytochemicals that reduce particle size and act as a capping agent [6]. Ag NPs (Fig. 2F), have fewer particles than Ag-Cu NPs (Fig. 2G), indicating a good infusion of Cu metal in Ag-Cu NPs. In Fig. 2F, the Ag NPs were uniformly monodispersed with a diameter of 11.9-15.1 nm and 14 nm average particle size. In Fig. 2G, the Ag-Cu NPs were polydispersed with a diameter of 22.9-31.4 nm and have a 27 nm average particle size. The capping of the produced NPs is confirmed by the scum surrounding them, as seen in Fig. 2F and 2G.

NPs formation using natural products

The preparations of NPs from different natural products are reported as listed in Table 2 [20-27]. The leaf extracts were used for preparation of NPs or their oxides, which were displayed significant antimicrobial, antioxidant, anticancer, dye remediation, etc. Cu and Ag NPs were prepared using *Cissus arnotiana* and *Origanum vulgare* extracts, respectively [26,27]. In particular, *P. cineraria* leaf extract was reported on Ag and Cu NPs preparation, and studied their antimicrobial and anticancer activities [1]. In present work,

bimetallic NPs is prepared from waste aqueous pod extract, and it is used as catalyst for epoxidation reaction. In addition, Ag and Ag-Cu NPs are displaying significant antimicrobial activities.

Application of green synthesized Ag NPs and Ag-Cu NPs

Antimicrobial activity

Three bacterial strains, i.e., *E. coli, B. subtilis*, and *S. cerevisiae* were examined with a 0.0038-0.5 mg/ml concentration range of Ag and Ag-Cu NPs using the disc diffusion method (Fig. 3A-C, Fig S2). Ag NPs have a higher inhibitory impact than Ag-Cu NPs at all concentrations. *B. subtilis* was the most susceptible to Ag NPs at 0.5 mg/ml concentration with a maximum ZOI of 85% (Fig. 3A), whereas *E. coli* and *S. cerevisiae* exhibited 73% (Fig. 3C) and 71% (Fig. 3B), respectively. Ag-Cu NPs (0.5 mg/ml) inhibited *B. subtilis* 60%, *E. coli* 20%, and *S. cerevisiae* 50%. At lower concentrations, Ag NPs (0.0321 mg/ml) inhibited *S. cerevisiae* by 42.85% (Fig. 4B), while Ag-Cu NPs (0.0156 mg/ml) inhibited it by 33.98% (Fig. 4B). Similar results are observed in Fig. 4D showing the energy kinetics of NPs against selected bacteria at 24 h and 48 h. The increasing order of potency of Ag NPs at high concentrations against microbes was *B. subtilis > S. cerevisiae > E. coli.* Ag NPs were most effective than Ag-Cu NPs against test microorganisms. Previous studies revealed that plant-derived metal NPs were employed against several pathogens and played a key role in drug delivery [28,29]. Feng et al. reported that reactive oxygen species which trigger cell self-destruction are formed when Ag NPs disintegrate into Ag^+ ion, inactivating the respiratory enzymes [30].

Epoxidation potential

Further, both the NPs were utilized for epoxidation of monoterpenoids using hydrogen-peroxide as a green oxidant. For the case study, linalool is taken as substrate and reacted with both the NPs at fixed reaction conditions (SI) listed in Fig. 5B1 & 5B4. The results showed high activity of Ag-Cu NPs in terms of conversion and product selectivity, indicating a major role of Cu in epoxidation activity and selectivity. Fig. 5B1 showed linalool conversion percentage with varying time (30-210 min), where, both NPs attained maximal conversion in 30-120 min. At 120 min, Ag NPs was displayed 65% conversion, while Ag-Cu NPs was converted to 88%. Up to 210 min, only 2-3% of additional conversion was noticed. Fig. 5B4 showed the product selectivity percentage of Ag and Ag-Cu NPs, where Ag-Cu NPs gave the highest selectivity towards 68% of 2-(5-methyl-5-vinyltetrahydrofuran-2-yl-propan-2-ol) (1b), and low selectivity towards 2-methyl-2-vinyltetrahydrofuran-5-one (12%) (1a), 2,2,6-trimethyl-6-vinyl tetrahydro-2H-pyran-3-ol (8%) (1c), linalool di-epoxide (2%) (1d). Product (1a) was obtained after over-oxidation of (1b), which may be due to high oxidant loading and elevated reaction temperature. While in case of Ag NPs, 1b was the major product (45%), and 1a (18%), as well as 1c (15%), were obtained in approximately equal proportions with linalool di-epoxide in minor percentage (5%).

Ag-Cu NPs were chosen for further optimization due to their high activity and selectivity. Using Ag-Cu NPs, the effect of temperature on linalool epoxidation was examined from 40-70 °C (Fig. 5B2). The graph showed maximal conversion (90%) at 50 °C in 150 min, however, at 60 and 70 °C, product selectivity

varied significantly. At 70 °C, the selectivity of 1b decreased as it is oxidized to 1a, increasing the selectivity of products 1a, 1c, and 1d (Fig. 5B5). Vilanculo et al. found that higher temperature favoured diepoxide production, and reduced the furan selectivity [31].

Further, the effect of oxidant loading on linalool epoxidation was studied using Ag-Cu NPs. As above, the ratio of substrate to oxidant loading (1:2) was effective for almost complete conversion with good selectivity. So, this ratio of substrate to oxidant loading at different concentrations are listed in Fig. 5B3, where an increase in linalool conversion percentage is observed on increasing the load from (1:1) to (1:2) (70-93%) after 210 min of reaction time, but the product selectivity is slightly comparable. While in case of 1:3 oxidant loading, the conversion percentage was nearly the same at 120 min, but the product selectivity was altered. The product 1a selectivity is decreased to 38%, and products 1c and 1d selectivity are increased to 20% and 25%, respectively (Fig. 5B6).

Also, the epoxidation of other monoterpenes like limonene, geraniol, α-pinene, and citronellol are studied using Ag-Cu NPs, and the results are presented in Table 3. From results, limonene is completely oxidized to produce 1,2-limonene oxide (2a) (54.5%) and 8,9-limonene oxide (2b) (38.6%), and dipentene dioxide (2c) (6.9%) in a minor amount (Fig. 5A). Limonene oxide has numerous uses in the polymer sector and has been explored as a technique for introducing CO_2 into polycarbonate production [32]. Similarly, α-pinene has double bond inside the ring, which preferably transformed to α-pinene epoxide as compared to the b-pinene [11]. These epoxides have ample use as flavouring agent due to enhance water solubility, lower volatility and organoleptically superior profile [33].

Conclusions

P. cineraria pod's waste water extract was utilized for the synthesis of Ag and Ag-Cu NPs. In this study, the characterization of NPs revealed their crystalline nature, stability, capping properties, and average sizes of Ag NPs (14 nm) and Ag-Cu NPs (27 nm). Ag NPs was showed high inhibitory activity (85%) against *B. subtilis*. Also, the epoxidation of linalool (monoterpenes) was achieved (93% conversion) using Ag-Cu NPs. Similarly, monoterpenes such as limonene, α-pinene, geraniol and citronellol are transformed through epoxidation (81–93%) to demonstrate the importance of utilizing these green synthesized NPs for the production of commercial important pharmaceutical active ingredients (API) and fine fragrances. The prepared Ag and Ag-Cu NPs are greener in nature, and have ample scope for using as anti-microbial agents with excellent catalytic properties for the selective oxidation. Ag-Cu NPs was successfully modified the model monoterpenoids such as limonene, geraniol, α-pinene, citronellol, and linalool to their corresponding epoxides for using as natural polymer as well as flavouring sectors.

Declarations

Acknowledgement

We are grateful to the Director, CSIR-CIMAP, Lucknow for providing the necessary laboratory facilities under the CSIR-Aroma mission (HCP0007, PE-II). The authors are thankful to SERB, DST for financial grant (CRG/2021/002525) for carrying out this work. Dr. S Chaturvedi is thankful to DST for WOS-A fellowship (DST/WOS-A/CS-94/2021).

Authors' contribution

Prashant Kumar: Experimental, Data Acquisition, Writing-original draft; Praveen Kumar Sharma: Experimental, Data Acquisition, Writing-original draft; Suman Singh: Writing (Biological part); Shivani Chaturvedi: Conceptualization, Supervision, Writing; Shreya Tripathi: FT-IR analysis; Huma Fatima: TEM analysis; Minakshi Grover: Microbial analysis, Supervision; Priyabrat Mohapatra: Methodology, Validation, Visualization; Prasant Kumar Rout: Methodology, Validation, Investigation, Funding acquisition, Writing - Review & Editing.

Funding

The work was financially supported by the Science and Engineering Research Board, DST, India with grant number CRG/2021/002525. Dr. S Chaturvedi is received financial support from DST, India in the form of WOS-A Fellowship with award number DST/WOS-A/CS-94/2021.

Ethical Approval

The manuscript is approved by the institute internal publication committee with communication no CIMAP/PUB/2022/68 for publication.

Conflict of interest. There are no conflicts to declare

Availability of data and material

The quality and reproducibility of the catalytic experiments for epoxidation of monoterpenoids were verified by triplicate analysis of the experiments and the results reported in this article correspond to the average of these measurements. The synthesis of NPs procedure and their associated antimicrobial activities reported is truthful, and no details are omitted that allowed the obtaining of these materials as they are reported in this manuscript. The spectroscopic measurements made are kept in their original files.

References

1. U. Jinu, M. Gomathi, I. Saiqa, N. Geetha, G. Benelli, P. Venkatachalam, Microb. Pathog. 1. **105**, 86 (2017).
2. G. Benelli, Parasitol. Res. **115**, 23 (2016).
3. D.K. Vizhi, N. Supraja, A. Devipriya, N.V.K.V.P. Tollamadugu, R. Babujanarthanam, Adv. Nano Res. **4**, 129 (2016).

4. H.S.A. Afifi, I.A. Al-rub, *Prosopis cineraria* as an unconventional legumes, nutrition and health benefits. In J. C. Jimenez-Lopez and A. Clemente (Eds.), *Legume seed nutraceutical research* (Intech Open, 2018). https://doi.org/10.5772/intechopen.79291.
5. S. Chaturvedi, P. Kumar, D. Kumar, N. Syed, M. Gupta, C.S. Chanotiya, P.K. Rout, S.K. Khare, Waste Biomass Valoriz. **13**, 3113 (2022).
6. Y. Periyasamy, B. Baskaran, V. Senniappan, S. Chidambaram, Mater. Res. Express **5**, 105402 (2018).
7. A.S. Anbu, P. Velmurugan, J.H. Lee, B-T. Oh, P. Venkatachalam, Inter. J. Biol. Macromol. **88**, 18 (2016).
8. P. Venkatachalam, P. Sangeetha, N. Geetha, S.V. Sahi, J. Nanomater. 2015 (2015). https://doi.org/10.1155/2015/753193.
9. C.M. Phan, H.M. Nguyen, J. Phys. Chem. A **121**, 3213 (2017).
10. S. Serra, D. De Simeis, Catal. **8**, 362 (2018).
11. N.J. Castellanos, H. Martinew Q, F. Martinew O, K. Leus, P. Van Der Voort, Res. Chem. Intermediate. **42**, 4227 (2021).
12. A.W. Baur, W.M. Kirby, J.C. Sherris, M. Truck, Am. J. Clin. Path. **45**, 493 (1966).
13. V.V. Makarov, A.J. Love, O.V. Sinitsyna, S.S. Makarova, I.V. Yaminsky, M.E. Taliansky, N.O. Kalinina, Acta Naturae **6**, 35 (2014).
14. G. Manjari, S. Saran, S. Radhakrishnan, P. Rameshkumar, A. Pandikumar, S.P. Devipriya, J. Environ. Manag. **15**, 262 (2020).
15. T.M. Rosbero, D.H. Camacho, J. Environ. Chem. Eng. **5**, 2524 (2017).
16. C. Guo, H. Liu, J. Wang, J. Chen, J. Colloid Interface Sci. **209**, 368 (1999).
17. C. Baudot, C.M. Tan, J.C. Kong, Infrared Phys. Technol. **53**, 434 (2010).
18. S.A. Akintelu, F.A. Similoluwa, Stem Cells **10**, 30 (2019).
19. B.D. Cullity, Elements of X-ray diffraction. Addison-Wesley Publishing Inc, USA (1956).
20. J. Jeevanandam, Y.S. Chan, M.K. Danquah, New J. Chem. **41**, 2800 (2017).
21. D. Mahendiran, G. Subash, D.A. Selvan, D. Rehana, R. Senthil Kumar, A.K. Rahiman, Bio Nano Sci. **7**, 530 (2017).
22. S. Rajeshkumar, S. Menon, S. Venkat Kumar, M.M. Tambuwala, H.A. Bakshi, M. Mehta, S. Satija, G. Gupta, D.K. Chellappan, L. Thagavelu, K. Dua, J. Photochem. Photobiol. B **197**, (2019). https://doi.org/10.1016/j.jphotobiol.2019.111531.
23. J. Santhoshkumar, S.V. Kumar, S. Rajeshkumar, Resour. Efficient Technol. **3**, 459–465 (2017).
24. M.R. Shaik, M. Khan, M. Kuniyil, A. Al-Warthan, H.Z. Alkhathalan, M.R.H. Siddiqui, J.P. Shaik, A. Ahamed, A. Mahmood, M. Khan, S.F. Adil, Sustain.**10**, 913 (2018).
25. J. Singh, V. Kumar, K-H. Kim, M. Rawat, Environ. Res. **177** (2019). https://doi.org/10.1016/j.envres.2019.108569
26. J.Y. Song, E.Y. Kwon, B.S. Kim, Bioprocess Biosyst. Eng. **33**, 159 (2010).
27. M. Sundrarajan, S. Ambika, K. Bharathi, Adv. Powder Technol. **26**, 1294 (2015).

28. A. Folorunso, S. Akintelu, A.K. Oyebamiji, S. Ajayi, B. Abiola, I. Abdusalam, A. Morakinyo, J. Nanostructure Chem. **9**, 111 (2019)
29. H. Fouad, H. Li, Y. Ding, E-S. Ahmed, A. Ghulam, J. Mo, Artif Cells Nanomed. Biotechnol. **45**, 1369 (2017).
30. Q.L. Feng, J. Wu, G.Q. Chen, F.Z. Cui, T.N. Kim, J.O. Kim, J. Biomed. Mater. Res. **52**, 662 (2008).
31. C.B. Vilanculo, L.C. de Andrade Leles, M.J. da Silva, Waste Biomass Valoriz. **11**, 1895 (2020).
32. F. Parrino, A. Fidalgo, L. Palmisano, L.M. Ilharco, M. Pagliaro, R. Ciriminna, ACS Omega **3**, 4884 (2018).
33. M. Kfoury, L. Auezova, H. Greige-Gerges, S. Fourmentin, Environ. Chem. Lett. **17**, 129 (2019).

Tables

Table 1
Comparison of yield of Ag and Ag-Cu NPs obtained via different wastewater extract obtained during preparation of *Prosopis cineraria* traditional dish.

[a] Samples *(Prosopis cineraria)*	Salt solution[a]	NPs (mg)[b]
Soaked	$AgNO_3$	205
	$AgNO_3$-$Cu(NO_3)_2$	268
Soaked + boil	$AgNO_3$	244
	$AgNO_3$-$Cu(NO_3)_2$	418
Washed + boil	**$AgNO_3$**	**458**
	$AgNO_3$-$Cu(NO_3)_2$	**710**
Boiled with traditional dish masala (Ker, kumtia, kamalkakdi and red chilli)	$AgNO_3$	187
	$AgNO_3$-$Cu(NO_3)_2$	258
[a]Concentration was noted after proper precipitation, washing and calcination.		
[b]Volume of waste water extract and concentration of $AgNO_3$ and Cu $(NO_3)_2$ was kept constant for each experiment.		

Table 2
Comparison of current work with previously reported work on green NPs synthesis.

S. No.	Plant	Part used	Type of NPs	Size (nm)	Application	References
1	*Amaranthus tricolor*, *Andrographis paniculata* and *Amaranthus blitum*	Leaf	MgO	18–28	Biomedical Field	[19]
2	*Psidium guajava*	Leaf	CuO	2–6	Dye Remediation	[20]
3	*Passiflora caerulea*	Leaf	ZnO	200–2000	Antibacterial	[21]
4	*Pongamia pinnata*	Leaf	ZnO	100	Antibacterial	[22]
5	*Aloe vera and Hibiscus sabdariffa lea*	Leaf	ZnO	9–18	Antibacterial, Antioxidant, Antiproliferative	[23]
6	*Diopyros kaki*	Leaf	Pt	2–12	-	[24]
7	*Cissus arnotiana*	-	Cu	60–90	Antibacterial, Antioxidant	[25]
8	*Origanum vulgare L.*	-	Ag	2–25	Antimicrobial	[26]
9	*Prosopis cineraria*	Leaf	Ag, Cu,	20-44.49, 18.9-32.09	Antimicrobial, Anticancer	[1]
10	Prosopis cineraria	**Pod waste water**	**Ag, Ag-Cu**	**14, 27**	**Antimicrobial, Epoxidation reaction**	**Current work**

Table 3
Testing of epoxidation activity of synthesized Ag-Cu NPs on other olefins substrate.

Substrate	Epoxidation Product[a]	Reaction condition	Conversion / Selectivity[b]
Linalool	Linalool epoxides (1a-1d)	10%Ag-Cu NPs, 210 min, 70 ^{o}C, Acetonitrile, linalool / H_2O_2 (1:2)	93/99
Limonene	Limonene monoxide	10%Ag-Cu NPs, 210 min, 70 ^{o}C, Dichloromethane, limonene / H_2O_2 (1:2)	93/98
Geraniol	Geraniol oxide	10%Ag-Cu NPs, 180 min, Acetonitrile, geraniol / H_2O_2 (1:2), 60 ^{o}C	86/92
α-Pinene	Pinene-oxide	10%Ag-Cu NPs, 250 min, Toluene, α-pinene / H_2O_2 (1:2), 70 ^{o}C	90/95
Citronellol	citronellol oxide	10%Ag-Cu NPs, 210 min, Toluene, citronellol / H_2O_2 (1:2), 50 ^{o}C	81/91
[a]Products were quantified by GC and GC-MS analysis.			
[b]Selectivity of products was calculated via the above-mentioned equation.			
Unlike linalool, limonene is a cyclic monoterpene having two alkene bonds which are oxidized to give limonene oxide with high environmental remediation applications, such as CO_2 capture.			

Schemes

Scheme 1 is available in the Supplementary Files section

Figures

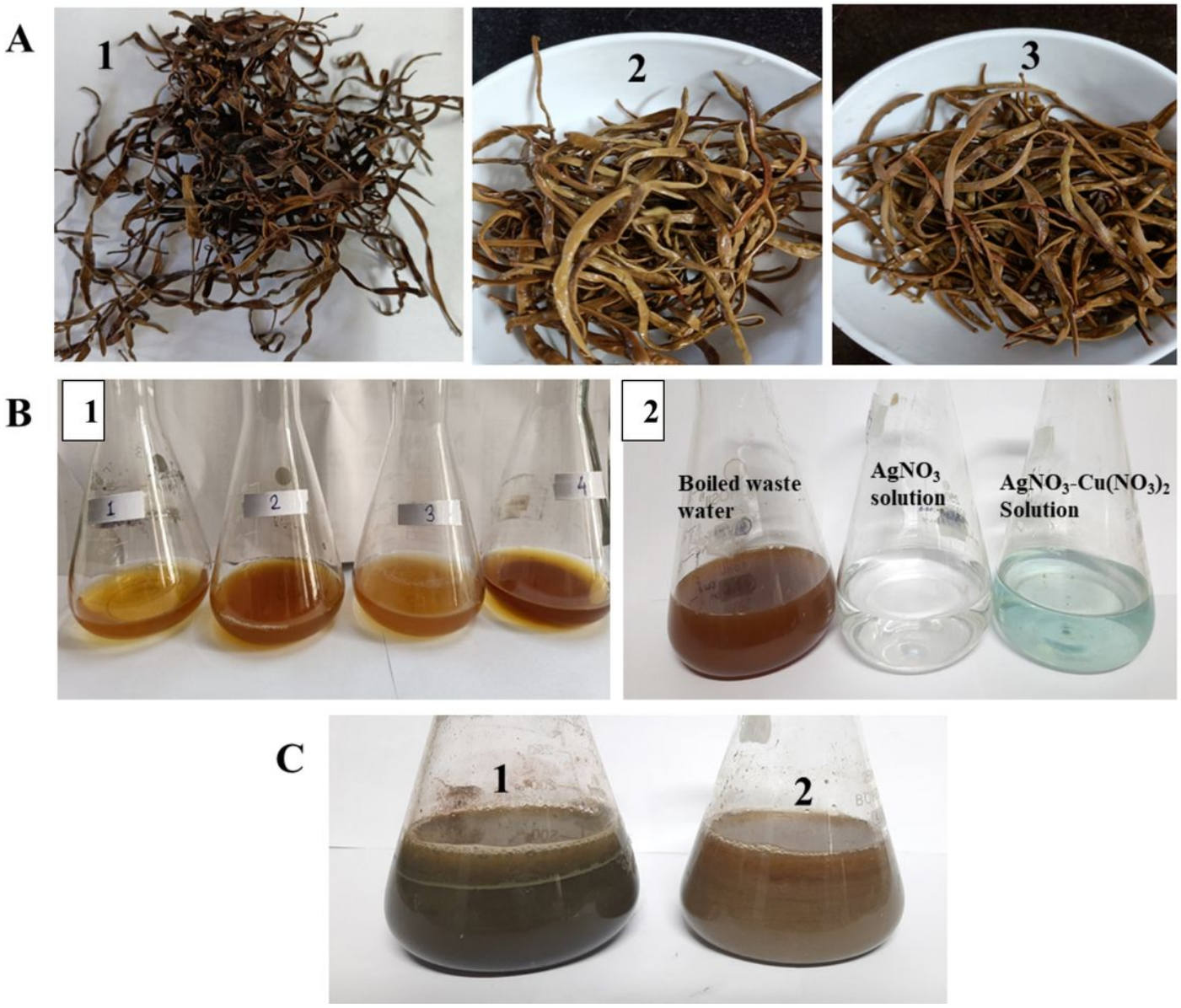

Figure 1

Different steps involved in NPs synthesis from *P. cineraria*. **A1**: Raw material of *P. cineraria*, **A2**: Soaked material **A3**: Boiled material; **B1**: Different treatments given to *P. cineraria* (1-4 as mentioned in Table 1), **B2** and **C**: Formation of NPs (brown (2) and olive-green precipitates (1))

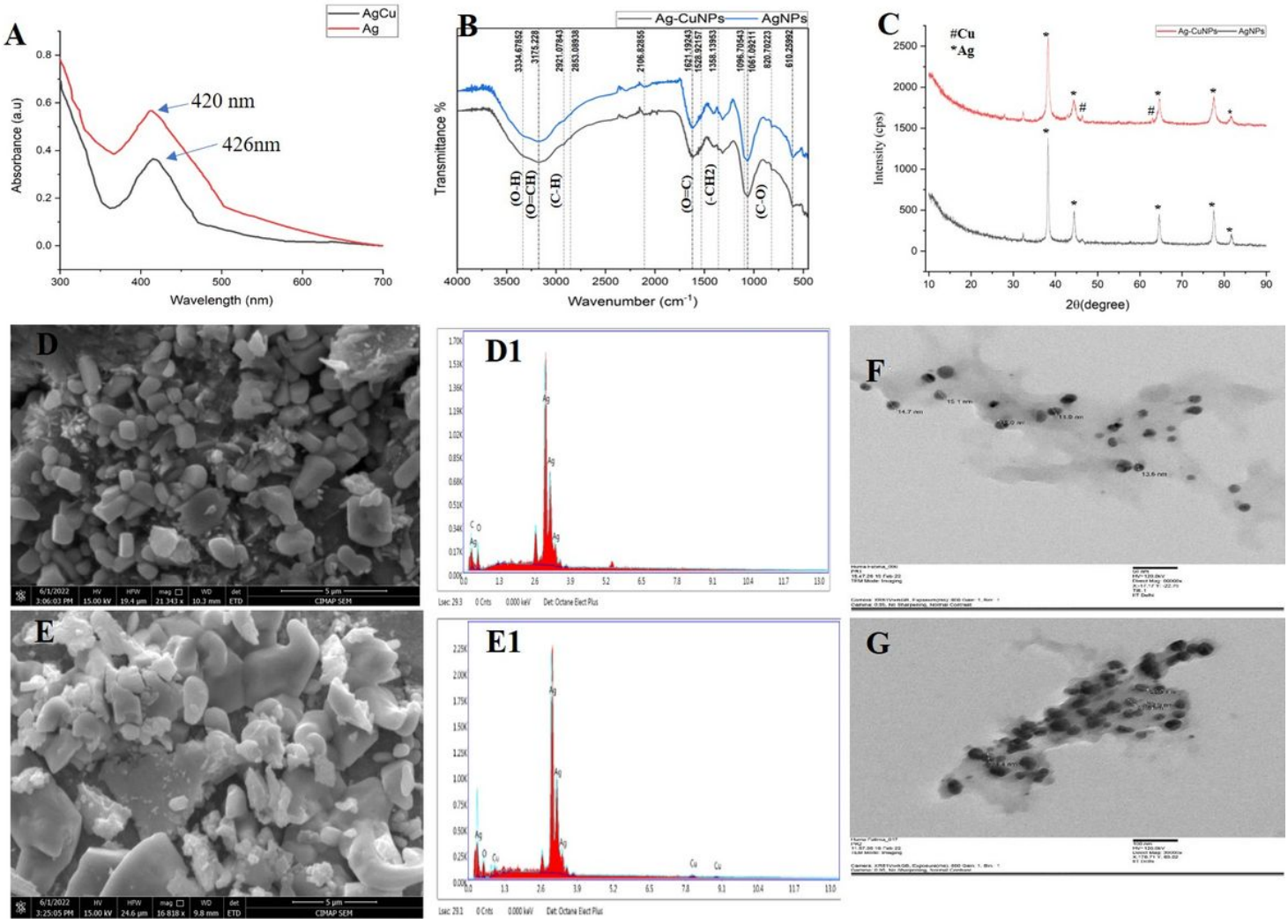

Figure 2

Physiochemical characterization of Ag and Ag-Cu NPs; **A**: UV-Vis spectrum of synthesized Ag (420 nm) and Ag-Cu (426 nm) NPs; **B**: FT-IR spectrum of synthesized Ag and Ag-Cu NPs; **C**: X-ray diffraction spectrum of synthesized Ag-Cu and Ag NPs showed high crystallinity; **D-D1** and **E-E1**: SEM-EDAX spectrum of synthesized Ag and Ag-Cu NPs; **F** and **G**: TEM spectrum of synthesized Ag and Ag-Cu NPs

Figure 3

Antibacterial activity of bio-synthesized NPs (S1: Ag-Cu NPs and S2: Ag NPs) against 3 different bacteria (*B. subtilis* (B), *S. cerevisiae* (S), and *E. coli* (E)).

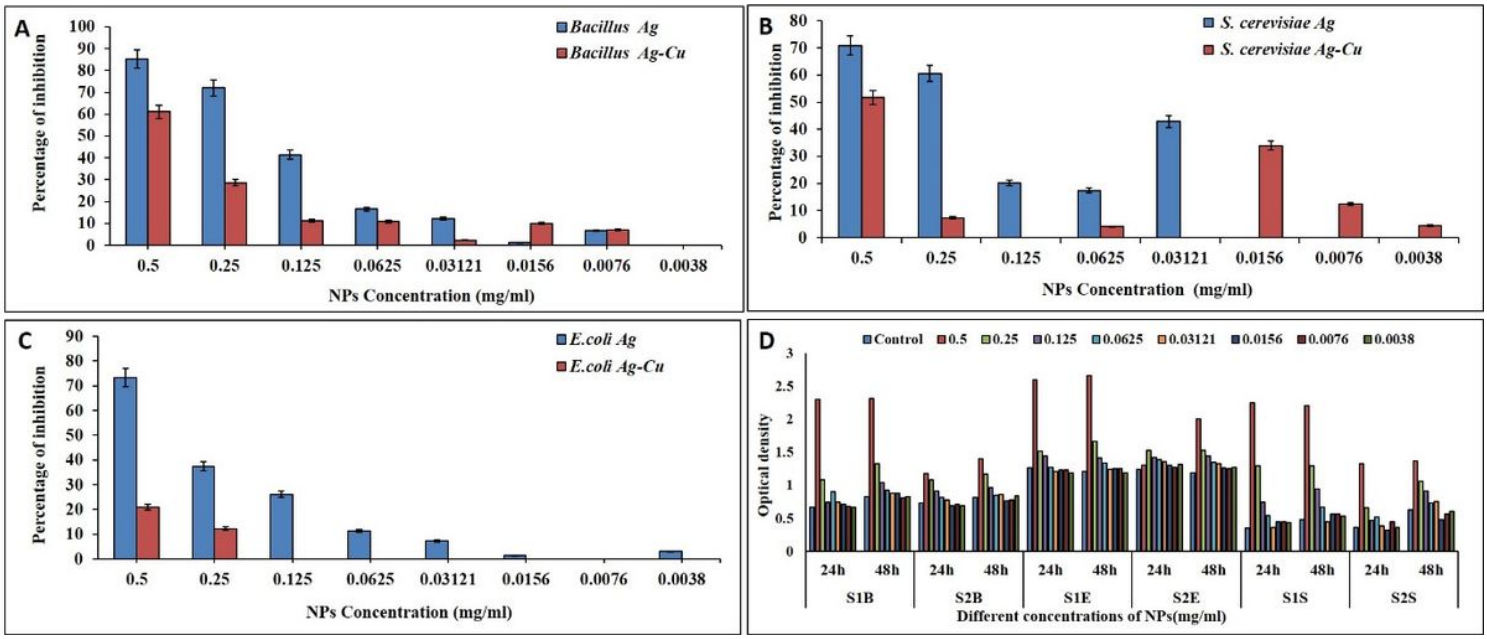

Figure 4

A-C Percentage inhibition of 3 bacterial strains (*B. subtilis, S. cerevisiae,* and *E. coli)* at different concentrations of Ag & Ag-Cu NPs; **Fig. 3D** Variation in optical density (OD) of 3 bacterial strains at different concentrations of Ag & Ag-Cu NPs; S1: Ag NPs, S2: Ag-Cu NPs; B: *B. subtilis*; S: *S. cerevisiae*; E: *E. coli*

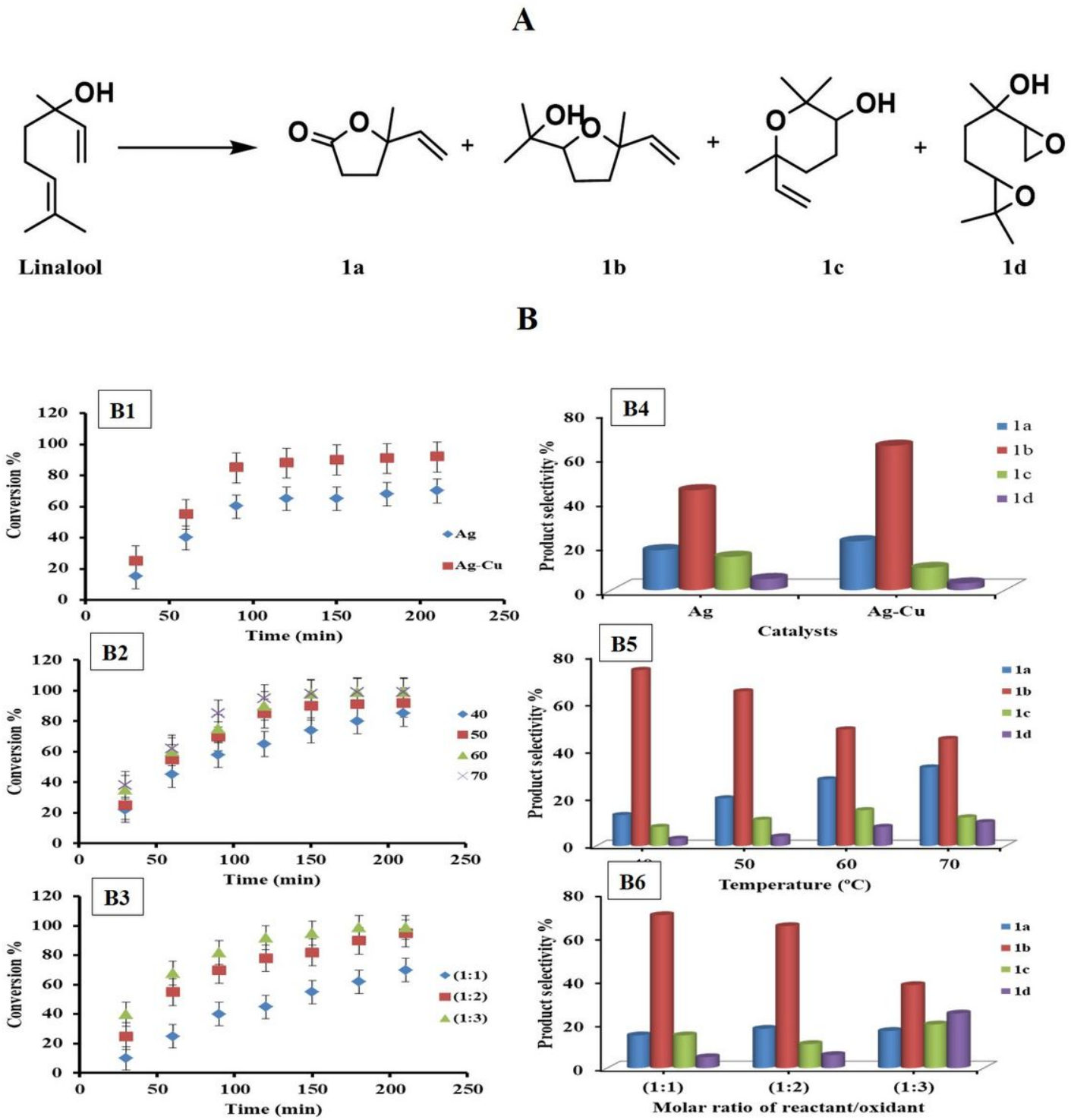

Figure 5

A Linalool epoxidation product distribution using Ag and Ag-Cu NPs; **Fig. B1 & B4** Conversion and product selectivity percentage of linalool epoxidation using Ag NPs and Ag-Cu NPs at fixed reaction condition (Ag-Cu NPs showed high epoxidation potential); **Fig. B2 & B5** Conversion and production distribution of linalool using Ag-Cu NPs at different temperature range. **Fig. B3 & B6** conversion and production distribution of linalool using Ag-Cu NPs at different substrate and oxidant ratio; 1a: 2-methyyl-

2vinyltetrahydrofuran-5one, 1b: 2-(5-methyl-5-vinyltetrahydrofuran-2-yl propan-2-ol), 1c: 2,2,6-trimethyl-6-vinyl tetrahydro-2H-pyran-3-ol 8%, 1d: linalool di-epoxide.

Supplementary Files

This is a list of supplementary files associated with this preprint. Click to download.

- Scheme1.jpg